The least cost design of 100% solar power microgrids in Africa: sensitivity to meteorological and economic drivers and possibility for simple pre-sizing rules

T. Chamarande, S. Mathy, B. Hingray

The least cost design of 100% solar power microgrids in Africa: sensitivity to meteorological and economic drivers and possibility for simple pre-sizing rules

Chamarande, T.[1,2,3,*], Mathy, S.[2], Hingray, B.[1]

1: IGE, CNRS, GINP, IRD, Université Grenoble Alpes, Grenoble

2: GAEL, CNRS, GINP, IRD, Université Grenoble Alpes, Grenoble

3: Schneider Electric, Grenoble

*Contact author: theo.chamarande@univ-grenoble-alpes.fr

Published in : *Energy for Sustainable Development*; 69 (2022) 211–223

https://doi.org/10.1016/j.esd.2022.07.001

Abstract

Autonomous micro-grids based on solar photovoltaic (PV) are one of the most promising solutions to provide electricity access in many regions worldwide. Different storage/PV capacities can produce the same level of quality service, but an optimal design is typically identified to minimize the levelized cost of electricity. This cost optimization however relies on technical and economic hypothesis that come with large uncertainties and/or spatial disparities.

This article explores the sensitivity of the optimal sizing to variations and uncertainties of such parameters. Using data from Heliosat and ERA5, we simulate the solar PV production and identify the least cost configurations for 200 locations in Africa.

Our results show that the optimal configuration is highly dependent on the characteristics of the resource, and especially on its co-variability structure with the electric demand on different timescales. It is conversely rather insensitive to cost hypotheses, which allow us to propose simple pre-sizing rules based on the only characteristics of the solar resource and electricity demand.

The optimal storage capacity can be estimated from the 75^{th} percentile of the daily nocturnal demand and the optimal PV capacity from the mean demand and the standard deviation of the daily power difference between solar production and demand.

Keywords: PV microgrids, microgrid sizing, Rural electrification, Levelized Cost of Electricity (LCOE), Africa

1 Introduction

The seventh Sustainable Development Goal of the United Nations is to "ensure access to affordable, reliable, sustainable and modern energy for all" [1]. Almost 550 million inhabitants do not have access to electricity in Sub-Saharan Africa and this number will increase with the fast demographic growth in this area [2]. Most of them are located in rural areas and in many cases, an affordable and sustainable electricity supply could help improving living conditions and developing local economies [1]. Fostering electricity access there requires large electrification programs, such as SE4all (Sustainable energy for all), the International Solar Alliance, the Terawatt Initiative or the Power Africa plan [3]–[6].

Such programs require governments and stakeholders (investors, researchers, manufacturers, …) to be guided toward the most interesting electrification strategy – which is expected to be region dependant [7]. In the recent years, a number of works have then estimated the cost-optimal options for different regions worldwide [8]–[12]. The choice, typically to be made between grid extension and micro-grid (MG) installation, is often based on the levelized cost of electricity ($LCOE$) [8], [13]–[16].

The $LCOE$ of a MG depends on many different features. It relies first on the technical configuration, e.g. the type of energy source or mix (e.g. diesel, photovoltaic, wind, hydroelectricity) and the required storage capacity of battery if any. Different MG configurations with different energy mix are then typically compared to identify the least-cost one. The cost-optimal configuration is expected to vary from one site to the other. When the MG is based on renewable sources, this configuration depends on the available resource and its variability (seasonality, day-to-day variability and low resource periods). This has been illustrated for 100% photovoltaic solar MG by Huld et al. [10] and Plain et al. [17].

The cost-optimal configuration for a site also depends on the socio-economical features of the system, for instance, the temporal profile expected for the electricity load, mainly determined by the different types of uses expected for the system. In a photovoltaic (PV) MG with batteries, less storage capacity is needed if the nocturnal load decreases, which is typically found when productive uses increase compared to domestic ones [9]. For a given PV installed capacity, a lower storage capacity results in a lower $LCOE$. The cost-optimal configuration also depends on the relative costs of the different technical components of the MG, e.g. costs of PV panels, converters, batteries.

A potentially critical problem for the identification of the cost-optimal configuration is that many features come with large variabilities, uncertainties or spatial disparities. The cost-optimal MG configurations, which have been estimated in a number of previous works, especially regarding electrification planning, are obtained using mean values for PV and battery costs. However, large costs variations are observed from one region to the other resulting from different country regulations, distribution circuits or local terrain constraints [18], [19]. Looking at a specific location, part of the unit costs can be well estimated but some other can come with large uncertainties: this is for instance expected to be the case for installation costs related to civil engineering, transportation or for maintenance costs related to the lifetime of the components, especially batteries as highlighted by [20], [21].

On the other hand, the costs of the different MG components can also significantly evolve with time, because of changes in country-specific costs due to regulations and taxes [22] and/or because of learning by doing: the large deployment and maturation of photovoltaic panels for instance led its price to be divided by almost 4 in 5 years [23]–[25]. These costs evolutions are expected to depend on the component of the MG. Learning rates for instance, defined as the relative unit cost reduction when doubling the installed capacity, were estimated around 23% for PV panels, 12% for on-shore wind

turbines and between 6% and 9% for lithium batteries [26], [27]. These evolutions are in turn expected to change the cost ratio between the components.

To our knowledge, the sensitivity of the cost-optimal configurations to cost hypothesis has not been characterized so far. Our first objective is to evaluate, for a generic 100% solar MG project in rural sub-Saharan Africa, the sensitivity of the cost-optimal MG configuration to the costs of the main MG technical components, namely the battery and the PV panels. In particular, this will allow to assess how the lowest cost MG configurations targeted for electrification or obtained in existing studies are modified with alternative component cost assumptions.

On the other hand, determining cost-optimal configurations is not straightforward. This is typically achieved with computation demanding simulations of the MG behaviour under a rather large number of different MG configuration scenarios requiring ad-hoc weather data, namely long time series of local weather and ad-hoc simulation models [28]. Such a simulation-based design process is not accessible to all operators especially in the context of a government or rural electrification agency tender where the profitability of MG over large areas needs to be estimated quickly. Simple pre-sizing rules, bypassing the need for simulations, are thus of high interest, for instance to discriminate between different solutions (MG, national grid, Solar Home Systems) or to assess a large portfolio of sites in rural electrification planning [8]. ECOWAS Centre for Renewable Energy and Energy Efficiency (ECREEE), International Energy Agency (IEA) and the Institute of Electrical and Electronics Engineers (IEEE) propose such rules for West Africa based on simple estimates of the demand and of the mean solar resource. These rules do however only target solar / diesel hybrid MGs [29], [30] or stand-alone PV systems [31].

The second objective of this paper is to test the possibility for simple rules for the pre-sizing of 100% PV MG systems. In Africa, the solar resource is indeed abundant and the large reduction in PV costs observed in the last decades makes such systems potentially highly competitive. 100% PV MGs produce moreover low greenhouse gases and air pollutant emissions compared to diesel generator and are not subject to fuel price volatility and supply difficulties [32]–[34]. This makes 100% PV MGs also very attractive as they will help countries to achieve the Nationally Determined Contributions (NDCs) they committed to fulfil during the 2015 Paris' Agreement [35]. However, contrary to solar / diesel hybrid MGs, where the electricity production can be adjusted at any time with less or more genset production, the quality service level that can be achieved with a 100% solar system, i.e. its ability to satisfy the demand at any time, fully depends on its design. To ensure reliable energy with such systems, the development of robust sizing rules is thus obviously key.

Section 2 details the data and hypothesis considered for the study as well as the methodology used to estimate the least cost MG configuration. The robustness of the least cost configuration to cost variations and their effects on the $LCOE$ is presented for different shapes of load profiles in section 3. This section also presents and evaluates simple rules to design the storage capacity and the size of the PV field of 100% PV micro-grids. Results are discussed in section 4 and the main conclusions are summarized in section 5.

2 Methodology

In the following, we consider a fictious MG system, where the power production, obtained from PV panel only, can be temporarily stored in batteries. The analysis is carried out for 200 different locations randomly selected in Africa (Figure 1). Some of them will be used for illustrative purpose when relevant.

For each location, the MG configuration is optimized to achieve a prescribed level of quality service with the lowest possible $LCOE$. The optimization is obtained thanks to simulations of the system behavior over a multiple year period. For any PV capacity/ storage capacity configuration, we simulate the PV production from local weather data and the storage cycles required to best meet a given demand profile, prescribed for the whole simulation period. The different steps of the simulations/optimization process are described in the following.

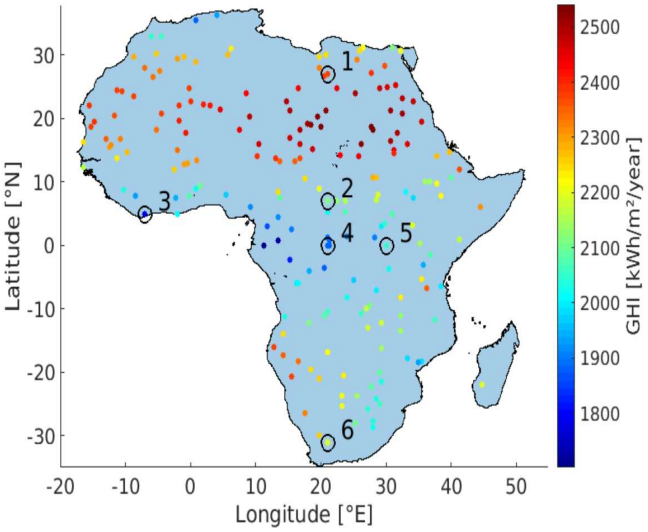

Figure 1 : Mean annual Global Horizontal Irradiance (GHI) for the 200 randomly selected locations. The six numbered locations will be used as examples to illustrate some results in the following. They have been chosen for their different resource characteristics (seasonality, day-to-day variability).

2.1 Load profile

Load profiles for microgrid projects are difficult to estimate, even with surveys [36]. We consider two hypothetic daily load profiles, representing domestic and productive uses (Figure 2). These profiles are derived from generic profiles considered in previous publications [37]. The domestic use profile is characterized by two peaks (morning + evening) and a quite low demand during the day. Conversely, the electricity demand only occurs during working hours during the day for the productive profile.

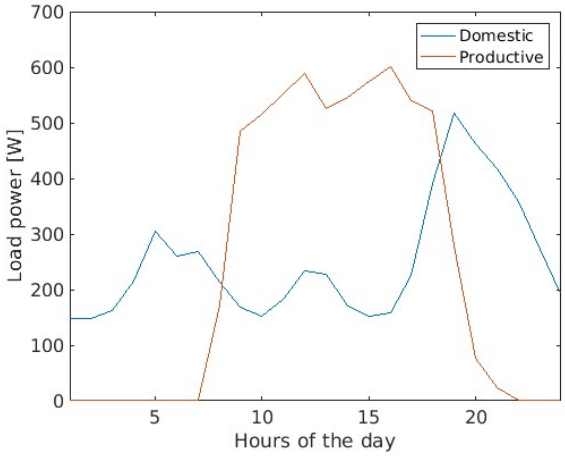

Figure 2 : Domestic and productive daily load profile

Seasonal variations in demand may occur especially for agricultural activities like irrigation or post-harvest processing which are common in many rural areas of Africa [38]. For the sake of simplicity, we model the seasonal profile of the energy demand as a sinusoidal function of time.

$$\overline{D}_d = \overline{D}(1 + A\cos\left(2\pi\frac{d - d_{max}}{365}\right)) \quad (1)$$

Where $\overline{D}_d$ $[Wh]$ is the daily energy demand of calendar day d, $\overline{D}$ $[Wh]$ is the annual mean daily energy demand, A is the half amplitude of seasonality and d_{max} is the calendar day for the maximum. In the following A is set to 0.5 and four seasonal profiles are in turn considered with a maximum daily demand occurring in January, April, July or October respectively. In addition, we also consider a non-seasonal profile, i.e. a profile where the daily electricity demand is the same throughout the year (cf. Figure 3).

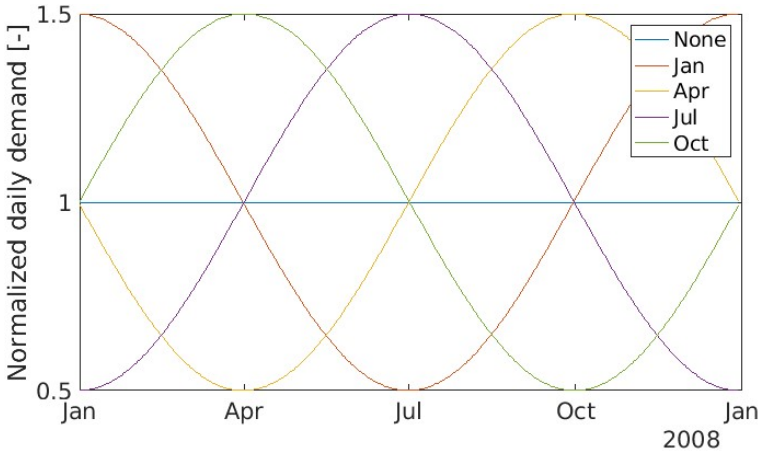

Figure 3 : The five seasonal patterns considered for the electricity demand

2.2 PV power production

The solar PV production in the MG is simulated at 15-min resolution for the 2008-2015 period using satellite derived solar irradiance from Heliosat SARAH2 [39] and temperatures from ERA5 meteorological reanalyses [40]. Irradiance data are available with a 0.05°x0.05° spatial resolution and ERA5 data with a 0.5° grid.

The electrical power delivered by the system (P_{AC} [W]) at a given time (t) is estimated from Global Tilted Irradiance (GTI $[W/m^2]$: global irradiance over an inclined panel) and module temperature T_m [°C] with the model of Lorenz et al. [41]. The model is described in equations (2) to (4):

$$P_{AC} = \eta \cdot (1 + \alpha\,(T_m - 25°C)) \cdot C_{PV} \cdot \frac{GTI}{1000\ W/m^2} \quad (2)$$

Where C_{PV} $[W_p]$ is the peak power of installed PV panels, $1000W/m^2$ corresponds to the irradiance at standard conditions, α is the sensitivity of panel efficiency to the module temperature T_m. The panel efficiency (η) accounts for inverter efficiency and for losses of the PV production system. Global tilted irradiance, the irradiance received by PV panels, is calculated as:

$$GTI = DNI \cdot \cos(\theta) + DHI \quad (3)$$

Where Direct Normal Irradiance (DNI: solar energy that reaches the surface in a straight line from the sun) and Diffuse Horizontal Irradiance (DHI: solar energy that has been scattered by particles in the atmosphere before reaching the surface) are derived from GHI based on the empirical method from Sandia National Laboratory [42] and where θ is the "effectiveness" angle, a function of solar angles (azimuth and zenith) and solar panel inclination and orientation. In the present work, PV panels are assumed facing south in the northern hemisphere and facing north in the southern hemisphere. As a rule of thumb, the tilt angle (inclination) is set equal to the latitude of the location [43].

The panel efficiency is typically considered to be a decreasing function of the module temperature. The sensitivity of the panel efficiency to temperature is here set to that of crystalline silicon cells ($\alpha = -0.0035\ /°C$). The temperature of the module (T_m) is estimated as a function of the ambient temperature (T_{amb}) and *GTI*, expressed as:

$$T_m = T_{amb} + \gamma \cdot GTI \qquad (4)$$

Where γ is a parameter related to the mounted type of the system (roof integrated, free standing…). We consider a mean value: $\gamma = 0.04\ °\mathrm{C}.\mathrm{m}^2/\mathrm{W}$.

2.3 Storage simulation

The storage/discharge cycles in the batteries of the MG are simulated as follows: the battery is charged when (1) the power production from PV panels is higher than the demand and when (2) the state of charge is below 100%. The battery is discharged when (1) production is lower than demand and when (2) the state of charge is higher than a minimum value set to 20% of the storage capacity. The same efficiency ($\eta_{storage} = 0.95$ [44]) is applied for charge and discharge sequences.

2.4 The sizing curve for a given quality service level

In our MG configuration, the demand is only supplied by the PV panels production and/or the batteries discharge. The multiscale variability of the solar resource makes it difficult to satisfy the demand at any time, one main challenge being to deliver electricity during periods with no solar resource (night) and with low solar resource (e.g. winter) (cf. [10], [17]). Satisfying the demand at any time would require provisioning significant storage and /or significant extra PV production capacity. This may in turn lead to costly and unaffordable systems. Following [10], [17], the design thus typically requires a compromise between the costs of the system and its reliability. In other words, a not fully reliable system, i.e. a system where the demand is not always fully satisfied, is targeted which allows reducing its size and thus its costs [17]. In this work, the systems are designed to achieve a prescribed reliability level; namely the hourly demand must be met 95% of the time. In other words, production may be lower than demand for 5% of the hours over the simulation period. This reliability level is based on the criteria of the Tier 5 in the multi-tier framework developed by ESMAP [45].

Different storage / PV panel configurations can produce the same level of quality service. The optimal design is identified to minimize the $LCOE$.

If a configuration is found suitable for a prescribed quality service level, configurations obtained by either increasing the PV capacity (the surface area of the PV panel array) or the storage capacity are also suitable. A minimal storage capacity is needed for each possible PV capacity. Conversely, a minimal PV capacity is needed for each possible storage capacity. The set of the least equipment configurations allowing for a prescribed level of quality service defines what we will refer to as the "sizing curve" for this level.

In the following, to ease the comparison between sites, the sizing curve is normalized using the annual mean power demand D_0. The sizing curve will next describe the relationship between the (normalized) storage capacity *S* and the (normalized) PV production capacity C_{PV} required to satisfy a demand D_0 with the prescribed level of quality service. Thus, the storage capacity S $[hrs_{eq}]$ is expressed in hours of equivalent demand ($1\ hrs_{eq}$ corresponds to the energy amount to supply one hour of electricity at the annual mean demand power D_0).

Due to the multiscale variability of the solar resource, PV panels do not always produce power at their rated power. The PV capacity C_{PV}^0 $[W_p]$, that would be required to produce over the whole period, an energy amount exactly equal to the total energy of a constant demand D_0 is thus greater than D_0. It is actually proportional to the inverse value of the so-called capacity factor *CF* of the PV panels for the considered site: $C_{PV}^0 = D_0 / CF$. Note also that the PV capacity C_{PV} $[W_p]$ required to achieve the desired level of quality service for a constant demand equal to D_0 is expected to be even larger than the "reference" capacity C_{PV}^0 discussed above. This needed PV "oversizing" is actually required to allow for enough production during the periods of low solar resource. In the following, the ratio $x = C_{PV}/C_{PV}^0$ is named the oversizing ratio of the PV system. It is dimensionless. For the seek of normalisation and comparison between locations, the sizing curve will finally relate the normalized storage capacity *S* and the oversizing ratio *x.* This normalized sizing curve obtained for a configuration where a level of quality service Q is further referred to as the $S_Q(x)$ function.

For any given location considered in the following, the sizing curve is identified from simulations. For a given normalized (PV capacity (oversizing ratio), storage capacity) configuration, a simulation consists of simulating 1) PV production, 2) storage operations (charge, discharge) over the whole period, and of 3) estimating the corresponding quality service level of the system. For different PV capacities in turn, simulations are used to identify the storage capacity value required to achieve the target quality service level (dichotomic identification).

2.5 $LCOE$ calculation and cost optimal mini-grid configuration

The least $LCOE$ MG configuration is finally identified from the $S_Q(x)$ curve as follows. For each (PV capacity, storage capacity) configuration, we use a simple economic modelling to estimate the total costs over the whole project lifetime and then the $LCOE$ of the system. The total costs of the project, *TC* in [€], have the following expression:

$$TC = C_S\alpha_S + C_{PV}\alpha_{PV} \tag{5}$$

where C_S and C_{PV} are the installed storage $[Wh]$ and PV capacity $[W_p]$ respectively and where α_S $[€/Wh]$ and α_{PV} $[€/W_p]$, the full unit costs of storage and PV respectively, simply read:

$$\alpha_S = Cost_S.\left(\sum_{k=0}^{int(\frac{L-1}{L_S})} \frac{1}{(1+d)^{kL_S}} + \sum_{k=1}^{L} \frac{P_{O\&M,S}}{(1+d)^k}\right) \tag{6}$$

$$\alpha_{PV} = Cost_{PV}.\left(\sum_{k=0}^{int(\frac{L-1}{L_{PV}})} \frac{1}{(1+d)^{kL_{PV}}} + \sum_{k=1}^{L} \frac{P_{O\&M,PV}}{(1+d)^k}\right) \tag{7}$$

where $Cost_S[€/Wh]$ and $Cost_{PV}$ $[€/W_p]$ are the unit investment cost associated to storage and PV panels respectively, where L, L_S, L_{PV} are the project, storage and PV panel lifetime respectively $[yrs]$ and where d is the discount rate $[-]$. The second term of each equation is related to the full cost contribution to cover maintenance and operation of the system where $P_{O\&M}$ is a proportionality coefficient between investment and cover maintenance costs $[-]$ (maintenance and operation costs are assumed to be time invariant and proportional to investment costs of each components).

Note that the total costs of the project can be also expressed as:

$$TC = C_s.\alpha_S + x.C_{PV}^0.\alpha_{PV} = \left(S_Q.\alpha_S + \frac{x}{CF}.\alpha_{PV}\right).D_0 \quad (8)$$

Where D_0 $[W]$ is the mean demand power, where *x* [-] is the oversizing ratio, where S_Q $[Wh/W]$ and C_0 $[W_p/W]$ are the normalized storage and reference PV capacities and where *CF* is the capacity factor introduced previously.

The $LCOE$ [€] for the considered MG has next the following expression:

$$LCOE = \frac{TC}{\sum_{k=1}^{L} \frac{D_{supply}}{(1+d)^k}} \quad (9)$$

where D_{supply} $[Wh]$ is the mean demand energy supplied each year by the system. It reads: $D_{supply} = Q.D_0 .8760$ where Q is the quality service factor achieved with the system (Q = 0.95 in the following). Merging equation 7 and 8, the $LCOE$ then simplifies to

$$LCOE = \frac{\left(S_Q.\alpha_S + \frac{x}{CF}.\alpha_{PV}\right)}{Q\sum_{k=1}^{L} \frac{8760}{(1+d)^k}} \quad (10)$$

The *LCOE* depends thus on 2 technical design variables, the normalized storage capacity S_Q and the PV oversizing factor x. For any given value of x, the sizing curve $S_Q(x)$ gives the normalized storage capacity required to achieve the target quality service level. The $LCOE$ can also thus be expressed as a function of x only.

Two limiting configurations from the sizing curve are to be noticed. When x tends to infinity, i.e. when the PV production capacity tends to infinity, the storage capacity tends to a minimum strictly positive value. Whatever the production capacity, a non-zero storage is indeed needed to move part of the diurnal production to the nocturnal electricity demand. As a result also, when x tends to infinity, $LCOE$ thus tends to be a linear increasing function of x.

If the battery system was perfect (with no energy losses in storage/discharge cycles), the other limiting configuration would roughly correspond to x = 0.95. This would correspond to the configuration where all the production could be used to satisfy 95% of the demand. This configuration would obviously require that a huge (and unrealistic) storage capacity is available (e.g. seasonal storage) to allow for the temporal redistribution of the production from resource rich periods to resource poor ones. In practice, the minimum value of the oversizing ratio x is greater than 0.95 because of storage losses that result from smaller than 1 storage efficiency. As mentioned above, for this minimum x value, the storage gets a typically very large value.

In practice, the minimum value for $LCOE$ is therefore reached for $x = x^*$ > 0.95 where:

$$\frac{\partial LCOE}{\partial x}(x^*) = \frac{\left(\frac{\partial S_Q}{\partial x}(x^*)\alpha_S + \frac{\alpha_{PV}}{CF}\right)}{Q\sum_{k=1}^{L}\frac{8760}{(1+d)^k}} = 0 \quad (11)$$

The optimal x^* value follows the equation:

$$\frac{\partial S_Q}{\partial x}(x^*) = -\frac{\alpha_{PV}}{\alpha_S.CF} = -\frac{r}{CF} \text{ with } r = \frac{\alpha_{PV}}{\alpha_S} \quad (12)$$

The optimal oversizing value x^* and the optimal storage value $S^* = S_Q(x^*)$ depend only on CF and on the full cost ratio r.

It is not possible to derive an analytical expression for $S_Q(x)$. $S_Q(x)$ depends on the storage efficiency, the shape of the load profile, the temporal variability structure of the local solar resource and the chosen quality service level. As mentioned previously, $S_{95}(x)$ was here estimated for each location by simulations.

2.6 Statistical distributions of costs for PV and batteries

The full costs of batteries and photovoltaic panels vary from one country to another due to different political, regulatory or institutional contexts, from one region to another due to local constraints and specific transport costs depending on access facilities. In addition, each type of investor has its own profitability objectives and its own perceptions of the risks inherent in each project. This leads to the use of specific discount rates that strongly impact the LCOE [18], [19], [46], [47]. The costs of batteries and photovoltaic panels are also expected to decrease over time as a result of learning by doing [23], [26], [48]. Cyclical effects may also occur, e.g. pressures on equipment production capacity or on materials that may drive prices up more or less temporarily.

In the following, we explore how robust the optimal design is to economic hypotheses. To do this, we rely on a statistical distribution of full costs estimated via Monte-Carlo simulations. For storage, the values of the different variables in Eq. (6) (storage costs, battery lifetime, project lifetime, discount rate, proportionality coefficient for O&M costs) are randomly sorted from their respective statistical distributions allowing in turn to give one estimate of the storage full costs. This simulation process is repeated 10'000 times to produce a probability density function (PDF) of the full costs for storage. The same process is applied for calculating PV full costs. Due to the lack of information and for the sake of simplicity, the different variables in Eq. 6 (resp. Eq. 7) are assumed independent and the PDF of each variable is modelled with a normal distribution. The mean and variance of each PDF (cf. Table 1) have been estimated so that the 10th and 90th of the PDF correspond to the range of values given by the IRENA (International Renewable Energy Agency) for 2015 and 2025 [19], [25], [44]. These estimations are based on a bottom-up analysis of the different technologies implied in PV and storage systems and an estimation of the learning cost curve for these technologies. Due to the lack of information, the PDFs for the O&M costs proportionality coefficient and the discount rate are assumed to be the same for both periods.

Variable	2015		2025	
	Mean	Standard deviation	Mean	Standard deviation
Storage investment costs $Cost_S$ $[\$/Wh]$	1.1	0.1	0.9	0.1
PV investment costs $Cost_{PV}$ $[\$/W_p]$	1.8	0.5	0.8	0.2
Storage lifetime L_S $[yrs]$	5	0.7	6.7	0.9
PV lifetime L_{PV} $[yrs]$	20	1.7	20	1.7
Proportionality coefficient for O&M costs $P_{O\&M}$ $[-]$	0.02	0.003	0.02	0.003
Discount rate d $[-]$	0.08	0.01	0.08	0.01

Table 1 : Economic parameters and component lifetimes distribution. The PV related parameters (investment cost and lifetime) are obtained from [25] and the storage ones from [44]. Discount rate and Proportionality coefficient for operation and maintenance are obtained from [19].

The PDFs of the full costs for each unit of storage or PV (α_S and α_{PV}) and the PDFs of the cost ratio r resulting from the Monte Carlo simulations are presented in Figure 4. As highlighted in the figure, the full costs for both PV and storage are expected to decrease with time. The full costs for PV is however expected to decrease faster leading to a shift of the cost ratio distribution to lower ratio values.

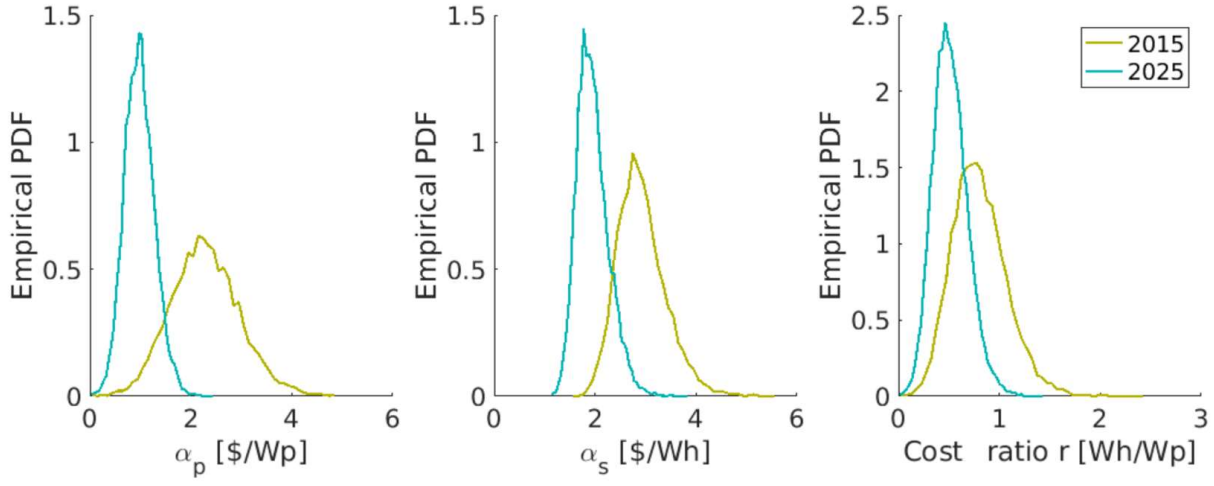

Figure 4 : Probability Density Functions of full PV costs (left), full storage costs (middle) and for the cost ratio r (PV/Storage) (right) as obtained from Monte Carlo simulations for two periods of time (2015 and 2025)

3 Results

3.1 Sizing curves for a 95% quality service level

For the sake of concision, the following sections (3.1, 3.2 and 3.3) only present results obtained for the non-seasonal demand profiles. Results for the seasonal demand profiles are presented in the Supplementary Material (Figures SM 1-10).

Figure 5 shows the $S_{95}(x)$ sizing curves obtained with the two daily load profiles of Figure 2, for 6 locations in contrasted climates (see Supplementary Material SM1 and SM2 for other locations).

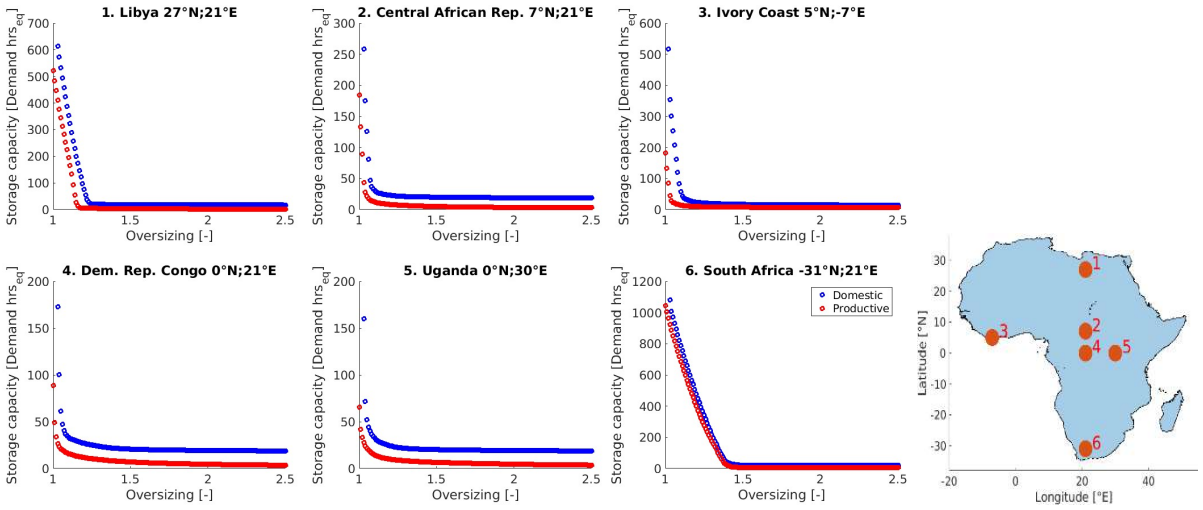

Figure 5 : Sizing curves $S_{95}(x)$ (normalized storage capacity S as a function of oversizing factor x) for six locations and for two demand profiles: domestic (blue) and productive (red) without seasonal variations. All MG configurations allow for a 95th quality service level.

Whatever the location and the load profile, the storage need is very sensitive to the oversizing value when the latter tends to 1. The large to very large storage needs obtained for an oversizing value close to one depend on the location and on the demand profile. When the size of PV panels is just enough to produce the yearly energy demand (i.e. $x = 1$) in average over the year, large to very large storage capacity is needed where the seasonality of the solar resource or of the demand is significant (cf. Supplementary Material SM1 and SM2). This allows to balance the energy from summer to winter or vice-versa (cf. Libya or South Africa). Much smaller storage values are needed for locations where the resource seasonality is small, as this is typically the case near the equator (cf. Central African Republic or Ivory Coast) (cf. Figure 5). This seasonal footprint is largely due to the latitude of the location, but this is not always the case. A significant resource seasonality is also observed in a number of equatorial locations because of significant seasonal variations of the nebulosity (cf. Uganda or Republic of Congo).

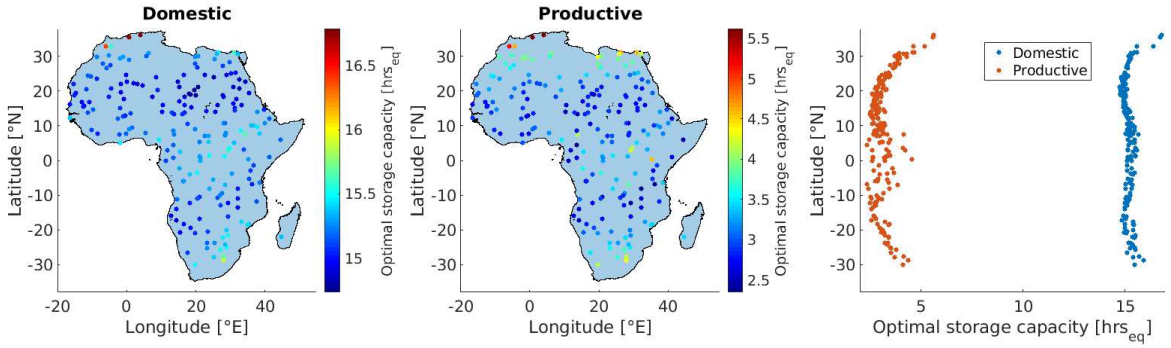

Figure 6 : Normalized storage capacities $[hrs_{eq}]$ for the 200 locations obtained with a large oversizing ratio (x = 2.5). (The normalized required storage capacity is the storage capacity [Wh] required per unit of mean power demand (i.e. 250 W) to satisfy the demand 95% of hours in a year. It is expressed in [Wh/W] or in $[hrs_{eq}]$. Left and middle maps: results for a domestic and a productive daily profile. Right: normalized storage capacities as a function of latitude (blue dots: domestic and red dots: productive, only a part of the abscissa (from 5 to 13) is not shown).

As mentioned previously, the storage capacity is expected to tend to a minimum value for large oversizing values (cf. illustration in Figure 6). The limiting value per unit of energy demand highly depends on the type of use. Whatever the location, it is larger for domestic uses than for productive ones (cf. Figure 6). It is actually always smaller than 16 hours in the first case and smaller than a few hours in the other. The storage is thus almost only required to deal with the sub-daily resource / demand mismatch, e.g. to move the energy produced during the day to the evening/night-time in the

domestic case. Another interesting point is that this minimum required storage value is almost always already reached for rather small PV oversizing values (values below 2.5) (cf. results for the 6 locations of Figure 5). For larger oversizing values, the required storage capacity decreases but the decrease is small and almost always less than one hour at mean demand power. For many locations, the storage is thus used for long temporal scale redistributions only when the oversizing value is small to very small.

For small oversizing values (below 1.5), the storage requirements are modified in a case of a seasonal demand. A larger seasonal resource / demand mismatch leads to a larger storage requirement (cf. Supplementary Material SM1 and SM2). For large oversizing values (above 2.5), the storage requirement almost no more depends on the demand seasonality.

3.2 Least-cost configurations

This section presents the least cost configurations obtained for the 200 locations with different demand profiles, a 20 years project lifetime and a cost ratio $r = 1$. The case of $r = 1$ is close to the most unfavourable cost configuration for PV for 2025 ($r = 1$ actually corresponds to the 99th percentile of the cost ratios distribution for this period). Estimating the oversizing values for $r = 1$ gives thus almost the minimum possible value of the optimal oversizing. In other words, the oversizing of a given project is very unlikely to be smaller than this value, whatever the cost-ratio configuration for the 2025 cost conditions.

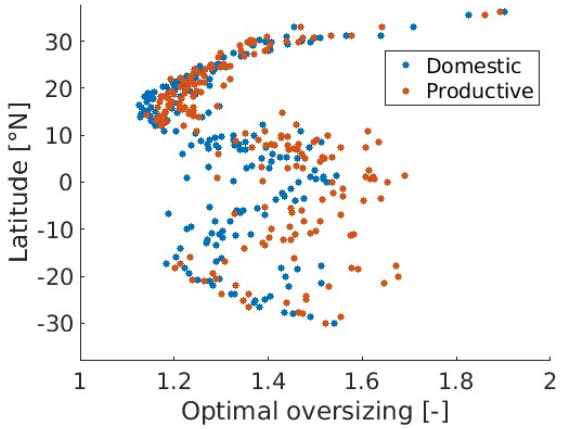

Figure 7 : Optimum oversizing x^* obtained by simulation with a cost ratio r=1 and without seasonality as a function of the latitude for a domestic (blue dots) and a productive (red dots) demand profile.

The PV optimal oversizing values as a function of latitude varies between 1.1 and 2 without major differences between the two daily load profiles. The optimal oversizing values are higher for regions with a high nebulosity (near the equator) or a high seasonality (north and south of Africa). The lowest values for optimal oversizing are obtained in the Sahelian part (around 15°N). Adding seasonality to the demand profile increases the optimal oversizing values but most of them stay below 2.1 (cf. Supplementary Material SM3 and SM4). This increase is larger when the peak demand occurs during the low resource period, which modify the shape obtained in Figure 7. When the peak demand occurs in the northern summer, the optimal oversizing values are lower in the north and higher in the south.

The required (normalized) storage capacities for the domestic profile are around 15 to 18 hours depending on the location (Figure 7). They are around 4 to 7 hours for the productive profile. Even with a cost ratio that favours large storage capacities ($r = 1$), these values are relatively close to the

minimal storage requirements from Figure 6. As for the optimal PV oversizing values, the optimal storage capacities are increased when adding seasonality to the demand, especially for the domestic load profile (cf. Supplementary Material SM5 and SM6). The demand / resource seasonal mismatch has a similar effect: when the peak demand occurs in northern summer, the optimal storage values are lower in the north and higher in the south. Note that whatever the type of use and seasonality, the required storage is smaller than 24 hours. The storage capacities for the domestic load profile could be perceived high for electrochemical storage, however these storage levels can be found in existing solar MG and they are much lower than what is proposed by the IEEE rule [31].

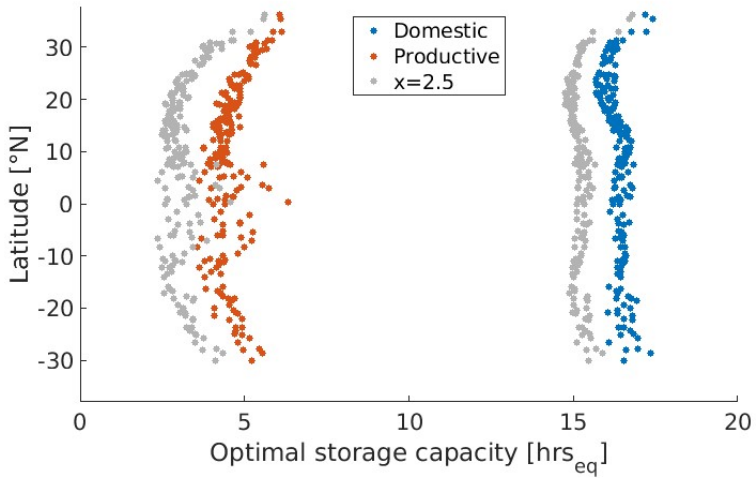

Figure 8 : Optimal normalized storage capacity S^* obtained by simulation with a cost ratio r=1 and without seasonality as a function of the latitude for a domestic (blue dots) and a productive (red dots) demand profile. Grey dots correspond to the limiting storage capacity requirement presented in figure 6 for x = 2.5.

The $LCOE$ values found here are in the same order of magnitude as the ones calculated by Nerini et al. [8] or by Szabo et al. in [13]. They are also logically higher than the $LCOE$ for electricity delivered by national grids with values below 0.1$/kWh for Zambia to 0.6$/kWh for Liberia but below 0.35$/kWh for most of the countries in Sub-Saharan Africa [49]. The $LCOE$ values we obtain are very sensitive to the sub-daily demand profile (cf. Figure 9). The $LCOE$ for a productive profile can be two to three times lower than the one for a domestic profile. This logically follows the much lower storage requirements that are two to three times lower in the productive case whereas PV capacities are similar in both demand configurations. The $LCOE$ evolution with the latitude is similar to the one found for the optimal oversizing values.

If the $LCOE$ is much less sensitive to the seasonality of the demand than to the sub-daily profile, a seasonal demand leads, for most locations, to larger oversizing values and storage capacities and, in turn to larger $LCOE$ values (cf. Supplementary Material SM7 and SM8).

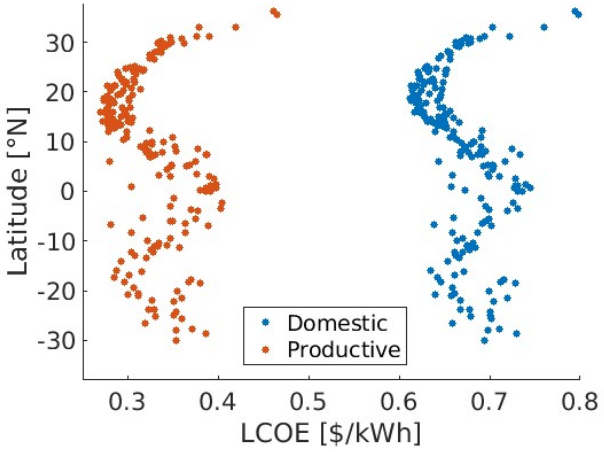

Figure 9 : Optimal LCOE obtained by simulation with a cost ratio r=1 and without seasonality as a function of the latitude

3.3 Sensitivity of the optimal configurations to cost ratio

As mentioned previously, the least-cost configuration depends on the cost ratio *r*. The PV oversizing level and the storage capacity of the least cost configuration is presented as a function of *r* for the six locations in Figure 10. Note that the variation range of cost ratios explored in the figure is larger than the variation ranges of the 2015 and 2025 distributions. For the sake of clarity, the 90% range of the 2015 and 2025 distributions is highlighted by the yellow and cyan vertical bands.

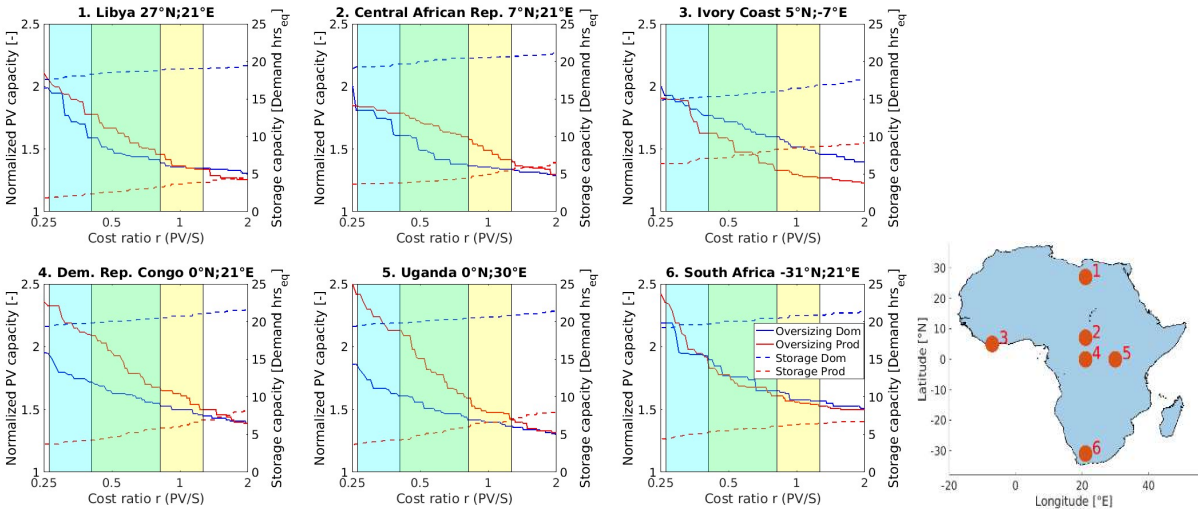

Figure 10 : Least LCOE configurations (normalized PV capacity (continuous lines; left scales); normalized storage capacity (dotted lines, right scales)) as a function of cost ratio (PV full costs / storage full costs, log scale) for six locations and for the domestic (blue lines) and the productive (red lines) load profiles. The 90% confidence interval of the cost ratio distribution is presented for 2015 (yellow vertical band) and 2025 (cyan vertical band). The green band corresponds to the overlap of cyan and yellow bands. All configurations allow for a 95th quality service level.

Larger r values (i.e. larger PV/S cost ratios) logically lead to smaller PV oversizing values and larger storage capacities.

For both variables, the range of the optimal design values is rather small. Considering the 200 locations, while the cost ratio varies by a factor of 8 (from 0.25 to 2), the optimal oversizing coefficient only varies

by a factor 1.5 for the domestic profile and of 1.7 for the productive one, for 90% of the locations. The ratio between the largest and the smallest possible PV oversizing value is always smaller than 2.

The robustness of the sizing of the storage capacity is even larger. Whatever the type of use, its variation range is often less than 10%. For both variables, the variation range is even smaller when the cost ratio is kept in the 90% variation range of the 2025 distribution (cyan vertical band). The optimal configuration is actually much more sensitive to the daily load profile than to the cost hypothesis. Even if optimal storage capacities and oversizing values are higher when adding seasonality to the demand, the robustness of the optimal configuration is similar to the one described here (cf. Supplementary Material and SM10).

As shown in Figure 3, the cost ratio *r* is expected to decrease in the coming years, which will further favour cost-optimal configurations with higher PV oversizing [25], [44]. In a longer term however, the cost ratio could increase again to values above 1 due to the learning-by-doing effects which are still expected to be significant for storage technologies [47]. Considering the lower sensitivity of the optimal configuration in the right-side of the oversizing curves in Figure 10, this would lead in turn to an increased robustness of the optimal sizing.

3.4 The possibility for simple pre-sizing rules

As highlighted in previous sections, the optimal configuration reveals to be rather robust to cost assumptions and to almost only depend on the characteristics of the solar resource, the demand and their co-variability. This suggests that it might be possible to find simple sizing rules that would avoid the computationally demanding simulations of any simulation-based optimization process.

We assess here the possibility for such a set of rules. These rules have been identified and tested from all the optimal configurations obtained, with the simulation methodology presented in section 2, for the 200 locations of Figure 1, the ten different load profiles presented in section 2.1 and four different cost ratios (namely 0.3, 0.5, 0.8 and 1 corresponding respectively to the quantiles 5%, 50%, 95% and 99% of the cost ratio distribution for 2025). The rules have been first identified/calibrated from half of the locations and their validity has then been assessed on the other half. The evaluation consists in comparing, for each location and each demand profile/cost ratio, the estimated optimal configuration and the reference one, i.e. the optimal configuration obtained with simulations. The detailed procedure to apply these rules can be found in Supplementary Material.

Two indicators are used for this evaluation: the normalized mean bias error (eq. (*13*)) and the normalized root mean square error (eq. (*14*)).

$$nMBE = \frac{1}{\bar{Y}} \sum_{i=1}^{n} \frac{Y - Y_{est}}{n} \tag{13}$$

$$nRMSE = \frac{1}{\bar{Y}} \sqrt{\frac{\sum_{i=1}^{n} (Y - Y_{est})^2}{n}} \tag{14}$$

With Y and Y_{est} the design values obtained for the considered variable (e.g. storage capacity, PV production capacity) for the reference configuration and with the simple rules respectively and $\bar{Y}$ the mean reference value obtained for the n =100 evaluations stations.

The rules apply for the normalized PV oversizing factor and the normalized storage capacity. As mentioned in the "Method" section, the actual PV panel area and the storage capacity required for a given location can be simply obtained with those normalized variables from the mean daily demand and from the mean capacity factor of solar panels to be expected for the location. Whereas the mean capacity factor can be easily extracted from already published data sets (e.g. [50]), the mean daily demand has to be typically estimated from local surveys.

As mentioned previously, the required PV oversizing factor is related to the resource / demand temporal mismatch. An indicator of this mismatch is the standard deviation (σ_{Diff}) of the daily power differences that can be estimated each day between the mean electricity demand and the mean PV production. This standard deviation obviously depends on both the mean daily difference and on the temporal variations of the difference. For the sake of simplicity, σ_{Diff} is here estimated from the time series of differences between the normalized daily demand (normalized by the mean annual daily demand D_0), and the normalized daily PV production for this day (production achieved without any oversizing of the PV panel area ($x = 1$) and normalized by D_0).

As shown in Figure 11, the variation range of σ_{Diff} depends on the seasonal profile of the demand. In the case of a non-seasonal profile, σ_{Diff} simply refers to the coefficient of variation of the solar resource, which derives from the joint effects of the seasonality of the Top Of Atmosphere (TOA) radiation and of the day-to-day variations of the atmosphere characteristics (e.g. nebulosity, aerosols). In locations with both small TOA radiation seasonality and low day-to-day weather variability (e.g. in the Sahel and a part of Angola), low values of σ_{Diff} are obtained (< 0.25).

In the case of a seasonal demand profile, the power difference variability is modulated. When the peak demand occurs in the high solar resource season, the value of σ_{Diff} can significantly decrease. For instance, a high energy demand in July in the Maghreb area makes σ_{Diff} decrease from 0.35 to 0.2. When the peak demand occurs in the low resource period, σ_{Diff} is expected to increase. In Maghreb, it can be higher than 0.5 for a high winter demand.

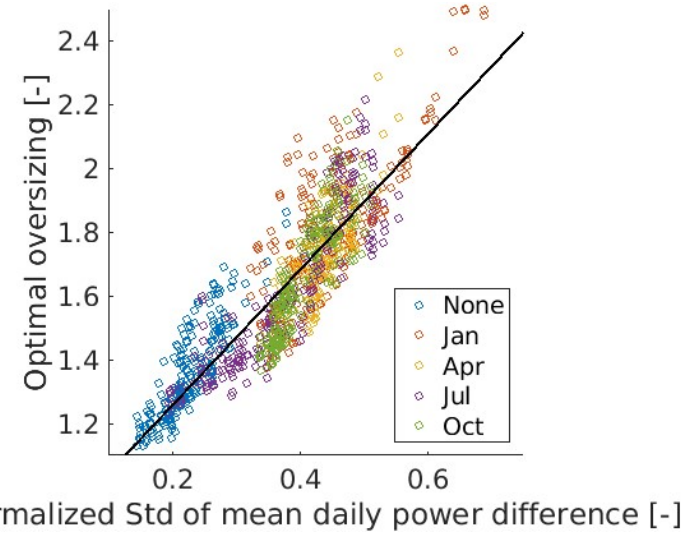

Figure 11 : Optimum oversizing x^* as a function of σ_{Diff}, the normalized standard deviation of the daily production/demand differences (differences estimated each day between the mean production and the mean demand for this day (the production is estimated with an oversizing factor of 1) and normalized by D_0). Results are presented for 5 different seasonal profiles of the demand (None: No Seasonality; Jan, Apr, Jul, Oct: Seasonality with a maximum in January; April, July and October respectively). This graph presents the optimum oversizing value for $r = 1$ and for both the domestic and productive load profiles (no distinction is made here between the 2 profiles).

As highlighted in Figure 11, regardless of the seasonality of the demand, the relationship between σ_{Diff} and the optimal oversizing x^* turns out to be strong, and a linear relation is expected to be a relevant first-order approximation.

$$x^*_{est,r=1} = 0.83 + 2.12\sigma_{Diff} \quad (15)$$

The nMBE and the nRMSE of this model stays respectively below 0.05 and 0.1 for each load profile (cf. Supplementary Material SM14). The global nRMSE for all categories is 0.07 which is quite good for such a simple rule.

The optimal normalized storage capacity was found to mainly depend on the sub-daily resource/demand mismatch (cf. Figure 12). It thus depends on the actual power production and in turn on the oversizing factor chosen for the system. For the storage capacity, the sizing rule is then based on the statistical distribution of the normalized nocturnal energy difference $E_{noct}\ [h]$ estimated each day between the load profile and the PV production profile of this day, where the PV production is obtained with the optimal oversizing x^*_{est} estimated by the previous rule (eq. (*15*)) and both production and demand are normalized by D_0.

For any given day, this normalized nocturnal energy difference reflects the energy that must be delivered by the storage during night-time. The normalized nocturnal energy difference is calculated between mid-time and mid-time the day after using equations (*16*) to (*18*).

$$E_{noct}(d) = \sum_{h=-12}^{h=12} P_{noct}(t) \cdot 1hr \quad (16)$$

Where $P_{noct}\ [-]$ is the normalized nocturnal power difference for each day t defined as:

$$P_{noct}(t) = \begin{cases} (D(t) - P_{AC}^{x^*}(t))/D_0, D(t) - P_{AC}^{x^*}(t) \geq 0 \\ 0, D(t) - P_{AC}^{x^*}(t) < 0 \end{cases} \quad (17)$$

Where $P_{AC}^{x^*}\ [W]$ is the power produced by PV panels with the optimal oversizing x^*_{est} obtained from equation (*15*) and $D\ [W]$ is the power demand. The sizing rule for the optimal normalized storage capacity S_{95}^* is considered as:

$$S^*_{95}{}_{est,r=1} = 0.93\frac{p_{75}(E_{noct})}{\eta_{storage}} + 0.14 \quad (18)$$

Where $p_{75}(E_{noct})\ [h]$ is the 75th percentile of the normalized nocturnal energy difference distribution and $\eta_{storage}\ [-]$ is the storage efficiency.

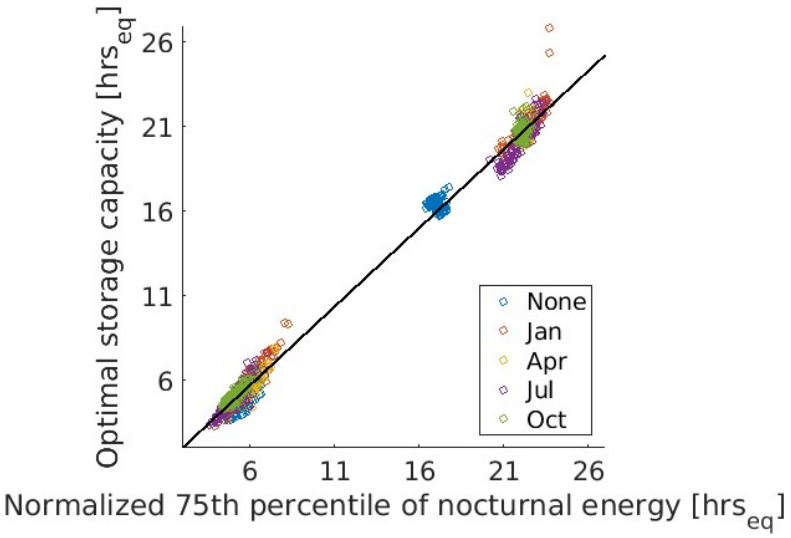

Figure 12 : Optimum normalized storage capacity S^* as a function of the 75th percentile of the normalized nocturnal energy $p_{75}(E_{noct})$. Results are presented for 5 different seasonal profiles of the demand (None: No Seasonality; Jan, Apr, Jul, Oct: Seasonality with a maximum in January; April, July and October respectively). This graph presents the optimum storage capacity values for $r = 1$ and for both the domestic and productive load profiles (no distinction is made here between the 2 profiles).

As highlighted previously in the manuscript, the storage requirement depends mainly on the load sub-daily profile. If all hours would have to be satisfied ($Q = 100\%$), the storage requirement would be related to the maximum nocturnal energy difference. In this work, we set a quality service $Q = 95\%$, which means that 5% of the hours can be unsatisfied. In this configuration, the 75th quartile of the nocturnal energy difference distribution turns out to be a very good predictor of the storage requirement.

For the storage capacity, the good order of magnitude is reached with this simple rule whatever the load profiles. If relative errors are much higher for the productive profile than for the domestic one (as a result of smaller absolute values of the required storage), absolute errors are most of the time lower than 1 hour of storage. The estimations for the optimal storage are very satisfactory with a global nRMSE below 0.04.

The level of quality service obtained with the estimated design does not always fit the level initially targeted (between $QS = 92\%$ and $QS = 96\%$ for 90% of the locations, cf. Supplementary Material SM13). An overestimated (underestimated) optimal storage capacity leads to a higher (lower) level of quality service and the same applies for the optimal oversizing factor. As the storage capacity is estimated from the estimated oversizing factor, the storage/PV under- and overestimations often compensate themselves. All in all, these compensations allow to have a good estimation of the $LCOE$ (cf. Figure 13).

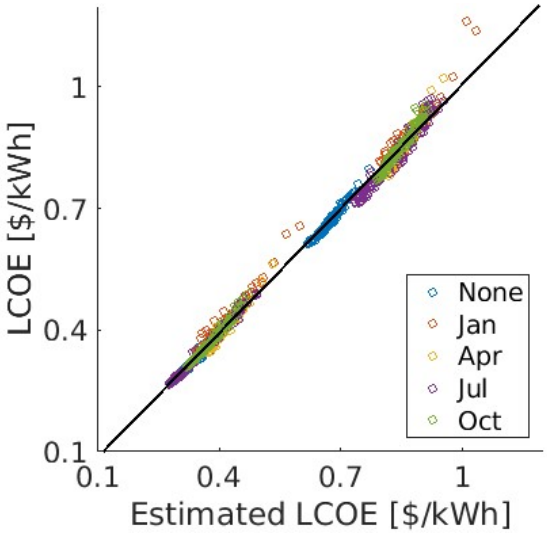

Figure 13 : Comparison between optimal LCOE obtained by simulation and configurations estimated by the sizing rule for all load profiles and $r = 1$

3.5 Pre-sizing rules for over cost ratios

The above results refer to a cost ratio of $r = 1$. As highlighted previously, the storage optimal capacity was found to be almost independent on the cost ratio value (cf. Supplementary Material SM 12 and SM 15). Whatever the actual cost ratio value, the storage capacity estimated with equation (*18*), calibrated for $r = 1$, is very satisfactory. The global nRMSE of estimates remains below 0.06.

Results obtained for the PV optimal oversizing conversely significantly depend on the cost ratio value. Smaller cost ratios lead to more favourable configurations for PV and thus to higher oversizing values (cf. Supplementary Material SM 11 and SM 14). An efficient way to account for this in the pre-sizing rules is to multiply the optimal oversizing estimated for $r = 1$ by a constant factor $f(r)$. This factor was estimated to be equal to 1.5, 1.2 and 1.1 for cost ratios equal to 0.3, 0.5 and 0.8 respectively.

$$x^*_{est,r} = f(r)\ .\ x^*_{est,r=1} \qquad (19)$$

When no correction is considered, i.e. when the relation (*15*) is used for the pre-design of the PV optimal oversizing for any value of the cost ratio, the global nRMSE is 0.18. With the correction introduced in equation (*19*), it decreases to 0.08, which becomes also very satisfactory.

Using equations (*18*) and (*19*), the level of quality service stays between 93% and 97% for 90% of all configurations (cf. Supplementary Material SM13).

A detailed description of nMBE and nRMSE related to optimal oversizing factors, optimal storage capacities and *LCOE* estimation for each cost ratio and load profiles can be found in Supplementary Material SM16. Even if the deviations between the estimated and the reference optimal configurations for the storage, the PV oversizing and the level of quality service can be non-negligible, the errors obtained for the $LCOEs$ are small whatever the cost ratios and the load profiles (global nRMSE around 0.02, cf. Figure 14).

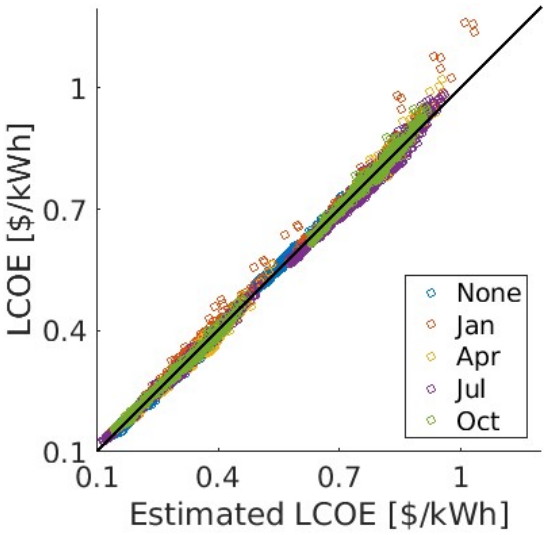

Figure 14 : Comparison between optimal LCOE obtained by simulation and configurations estimated by the sizing rules for the four cost ratios (0.3, 0.5, 0.8, 1) and all load profiles.

3.6 Summary of pre-sizing rules

The data, calculations and rules finally proposed in the present work for the pre-sizing of 100% solar MGs are summarized in the diagram of Figure 15. The details of each step are given in the Supplementary Material.

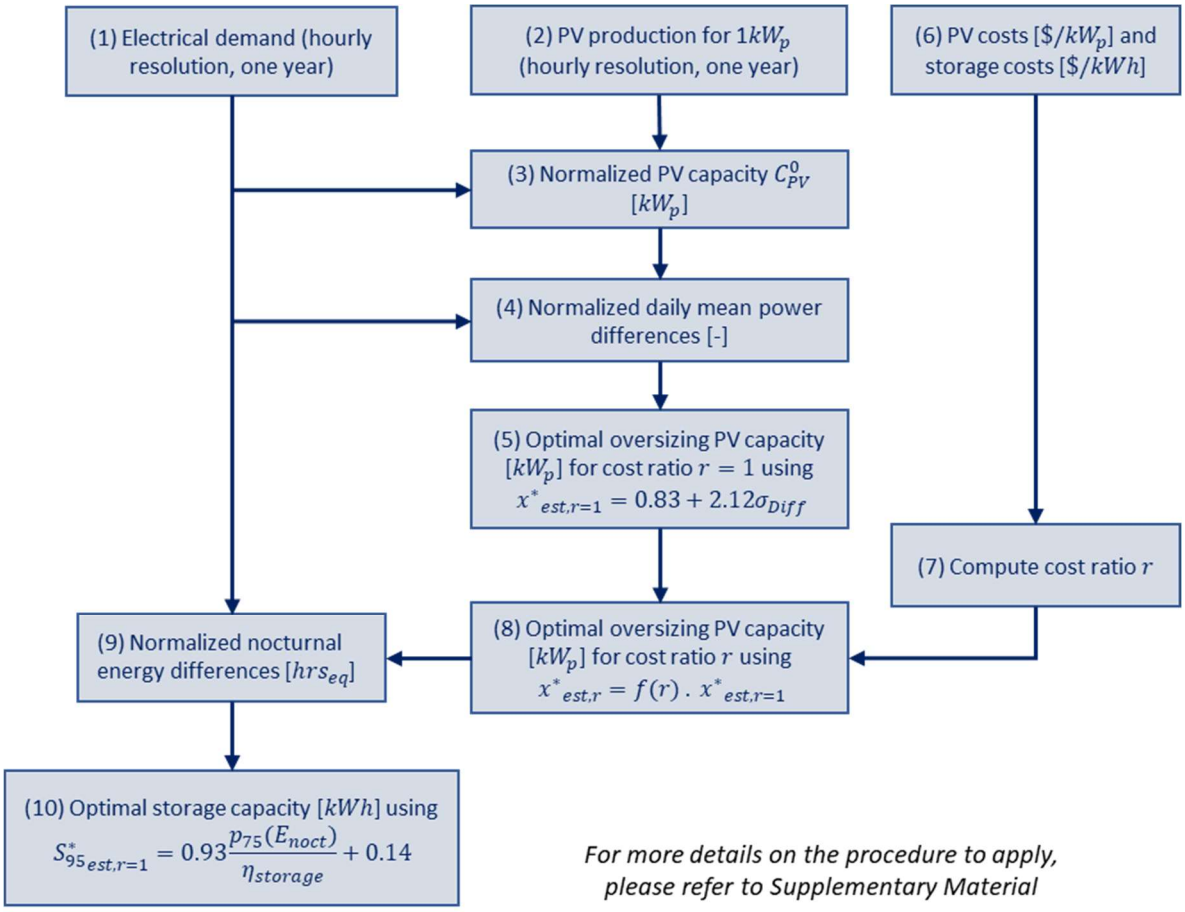

Figure 15 : Summary diagram of the procedure to apply the pre-sizing rules

4 Discussion

4.1 Influence of the load profile choice

As highlighted here and in some other publications, the load profile has an important influence on the optimal MG configuration. On the other hand, the load profile to be expected for a rural community is very uncertain *a priori* (cf. [36], [51], [52]). Having a good estimate of the load profile is thus obviously a key challenge and an important design issue. This however not modifies the relevance and impact of our analyses. On the one hand, an interesting finding of our work is indeed that the design is almost not sensitive to cost hypothesis. Our results additionally suggest that this applies whatever the load profile. Analyses with an intermediate daily profile (50% domestic/50% productive) give for instance similar (intermediate) results (cf. Supplementary Material SM 17 and SM 19). On the other hand, the simple design rules proposed here are expected to apply whatever the daily/yearly load profile. The characteristics of the load profile are indeed considered both (1) in the mean power difference between production and demand, that is used to estimate the optimal oversizing factor, and (2) in the mean nocturnal energy difference, that is used to calculate the optimal storage capacity.

4.2 Influence of technical/economic hypothesis and choices

Our results were obtained under a set of technical choices and economic hypothesis. How they might influence the optimal configuration, the LCOE and the robustness of the sizing rule would need to be studied.

For instance, the targeted level of quality of service is expected to impact the optimal configuration. A lower level would decrease the storage requirements and /or the PV installation size and would decrease in turn the battery and/or PV costs [17], [53]. The way the quality of service is defined is also expected to impact the design. This would probably be an issue for specific research.

Similarly, unit costs of PV and storage are expected to depend on PV panels and battery efficiency, on the minimum state of charge of the battery below which the battery should not fall. The possible effects of some of these features on the design are easily predictable. A higher value for the minimum battery state of charge would logically increase the storage requirement and in turn the storage costs. A smaller PV efficiency would similarly increase the required surface of PV panels and in turn PV costs.

A modification of unit costs and of their respective variation ranges would change the PV/battery cost ratio and its variation range. If the influence of such modifications would be worth investigating, our results are not expected to be significantly modified. Results obtained in Figure 10 are very similar when the variation range of r is extended to the range $[0.1\,,3]$: the robustness of the optimal configuration to modifications of the cost ratio is slightly smaller on the range $[0.1\,,0.25]$ but it is larger on the range $[2\,,3]$ (cf. Supplementary Material SM 19).

A more detailed modeling could be also considered to account for auxiliary costs such as costs of civil engineering, cost of the distribution grid and costs of distribution losses, etc. (cf. [54]). Some of those auxiliary costs are not expected to modify the optimal configuration of a 100% solar MG and are not expected to modify the pre-sizing rules discussed above. They would just result in the introduction of a fixed cost and increase in turn the $LCOE$ by a constant value. Another issue could be the influence of economies of scales, with lower unit costs for larger project sizes [55], or the influence of the

component lifetimes, which are very sensitive to maintenance quality, local weather conditions, charge/discharge cycles for the battery, degradations,… [20], [21].

4.3 Comparison with other sizing rules

As stated in the introduction, some international organizations propose rules or guidelines to design isolated MG in Africa.

In all cases, the load profile of the community has to be estimated based on the different appliances (light bulb, TV, fridge, …) to be used and on their respective consumption profiles. This allows in turn estimating the mean daily demand and the nocturnal energy consumption of the whole system.

The Institute of Electrical and Electronics Engineers (IEEE) [31] proposes a rule to size 100% PV systems that can be compared to our rule. The PV array is sized using the mean daily demand and solar resource for the worst month (high monthly demand and low resource). For the storage capacity, the IEEE recommends 5 to 7 days of autonomy to deal with sequences of low resource days. This leads to much larger $LCOEs$ (with storage capacities at least 5-8 times larger than the ones estimated in the present work).

Contrary to the IEEE, the International Energy Agency (IEA) [30] and the ECOWAS Centre for Renewable Energy and Energy Efficiency (ECREEE) [29] give rules to design hybrid PV/diesel MG. In such a configuration, the level of service quality that can be achieved is no more an issue, as the genset can supply the missing solar production at any time.

Similarly to the IEEE rule, the rule proposed by ECREEE [29] uses the mean daily demand and solar resource for the worst month to size the PV array but they recommend a smaller storage capacity corresponding to 2 times the value of the nocturnal energy consumption.

For the IEA [30], the design recommendations take the form of general guidelines: the installed PV capacity should be able to supply more than 20% of the daily energy demand and the storage capacity should be large enough to supply the nocturnal energy demand apart from the evening peak power that should be supplied by the diesel genset. A large part of the demand is thus expected to be supplied by the genset making the design of the PV / storage components rather simple.

The two previous rules apply to hybrid PV / diesel systems. They are not necessarily suited for remote locations where fuel supply is not reliable enough or for MG operators who want to use only decarbonized technologies. The rules we propose in the present work apply to 100% solar systems that could fit with the above constraints/objectives. Our results show that a 95% level of quality service can be reached with such systems, without any diesel generator and with smaller storage capacities than those proposed by the ECREEE. Our work additionally shows that the least cost configurations for such systems, very robust to a set of economic hypotheses, have to be adapted from one location to the other depending on the local climate features and on the sub-daily demand profile.

Our rules do not replace a more accurate sizing of a MG that could be done with HOMER [56] or any similar optimization software. It only aims at pre-assessing the regions where 100% PV MGs have a potential by quickly estimating the cost of power generation and compare it with other energy sources or other electrification solutions (national grid, solar home systems) for rural electrification planning. The sites for which this comparison favours a 100% PV MG will need to be studied in more detail.

5 Conclusion

The optimal configuration and the $LCOE$ of autonomous PV + battery systems is expected to depend on cost hypotheses. The robustness of the least cost configuration to cost assumptions is investigated for 200 African locations. The simulation-based design is carried out to achieve a prescribed level of quality service, namely to supply energy for 95% of the hours.

Whatever the shape of the load profiles (domestic or productive), we show that different storage / PV oversizing configurations are suited to achieve a prescribed level of quality service. The large storage requirements usually recommended can be reduced by oversizing the PV production capacity. In most of the cases, an oversizing coefficient of 2.5 is enough and the storage energy requirements are close to the value that allows to deal with the sub-daily resource/demand mismatch.

The least-cost configuration that allows to achieve a given level of quality service depends, among other drivers, on relative costs of PV and battery, but the sensitivity to the cost ratio is not large. The robustness of the configuration is thus rather good. When the cost ratio varies with a factor 8, the variations of the optimal oversizing factor are most of the time not larger than 70%, while the one for the required storage capacity are often smaller than 10%. The required storage capacity is thus highly robust to cost ratio variations.

The $LCOE$ for a productive load profile is two to three times lower than the one for a domestic load profile. This is an incentive for micro-grid designer to integrate as much productive uses as possible when assessing the electricity demand of a community. This definitively also calls scientists and practitioners to collect, share and publish demand data for a better knowledge of the temporal profile of the demand and its possible evolution through years.

All in all, the optimal (PV capacity / storage) configuration almost only depends on the characteristics of the solar resource, the electricity demand and their co-variability. This allows to propose simple rules for a rapid but reliable design. The goal of these rules is not to find the accurate optimal configuration for one specific site, it is rather to evaluate quickly the cost of electricity from solar MG over a large area. Such estimation can then be used to compare solar MG to different electrification solutions in a preliminary planning. The optimal oversizing factor can be estimated using the standard deviation of the mean daily power difference between the solar power production and the power demand. The required storage capacity can be calculated using the 75^{th} percentile of the daily nocturnal energy difference between the load profile and the solar power production. These rules give a good estimate of the optimal configurations whatever the load profile (domestic or productive, seasonal or not) and the cost ratio (between 0.3 and 1) considered.

The approach used in this work and the results offer further research perspectives. A least $LCOE$ criterion was used to determine the optimal configuration. It could be interesting to compare the results for this criterion obtained with our rule and with the ones proposed by the IEEE, the IEA and the ECREEE. This comparison should also consider the environmental impact of the MG (for instance, the greenhouses gases emissions, the land use or the toxicity to human health and to ecosystems) and modified rules could be derived by including these criteria in the optimization.

The methodology presented here was applied to identify the optimal (PV capacity/storage) configuration of 100% PV MGs. It could also be used for MGs based on other variable energy sources such as wind or hydroelectricity that are also promising renewable energy sources in many regions worldwide (e.g. [57]). For wind power and hydroelectricity, the important civil engineering works to be produced and the large variety of terrain configurations to be found would likely result in a large

variability of installation and in turn equipment costs. The robustness of the optimal design configurations is expected to be in turn rather low.

The demand profiles considered in this article are constant from one year to the other, however the evolution of the electricity demand during the lifetime of the MG could change the performance of the system. A better knowledge of the processes involved in the evolution of the electricity demand are necessary to choose the most suitable profile on which the sizing rules must be applied.

Author Contributions: conceptualization and methodology: T.C., B.H., S.M.; software, formal analysis, writing - original draft preparation: T.C.; writing – review and editing T.C., B.H. and S.M.

Conflicts of Interest: The authors declare no conflict of interest.

Acknowledgements: This work is part of a PhD thesis funded by the French Ministry of High Education, Research and Innovation and by Schneider Electric.

References

[1] United Nations, « UN Sustainable Development Goals », 21 janvier 2021. https://sdgs.un.org/goals/goal7
[2] International Energy Agency, « Africa Energy Outlook 2019 », 21 janvier 2021. https://www.iea.org/reports/africa-energy-outlook-2019
[3] SEforAll, « Sustainable Energy for All », 21 janvier 2021. https://www.seforall.org/
[4] ISA, « International Solar Alliance », 21 janvier 2021. https://www.isolaralliance.org/
[5] TI, « Terawatt Iniative », 21 janvier 2021. https://terrawatt.org/
[6] USA International Development, « Power Africa », 21 janvier 2021. https://www.usaid.gov/powerafrica
[7] D. Puig *et al.*, « An action agenda for Africa's electricity sector », *Science*, vol. 373, n° 6555, p. 616-619, août 2021, doi: 10.1126/science.abh1975.
[8] F. F. Nerini, O. Broad, D. Mentis, M. Welsch, M. Bazilian, et M. Howells, « A cost comparison of technology approaches for improving access to electricity services », *Energy*, vol. 95, p. 255-265, janv. 2016, doi: 10.1016/j.energy.2015.11.068.
[9] C. L. Azimoh, « Electricity for development: Mini-grid solution for rural electrification in South Africa », *Energy Convers. Manag.*, p. 10, 2016.
[10] T. Huld, M. Moner-Girona, et A. Kriston, « Geospatial Analysis of Photovoltaic Mini-Grid System Performance », *Energies*, vol. 10, n° 2, p. 218, févr. 2017, doi: 10.3390/en10020218.
[11] J. F. Alfaro, S. Miller, J. X. Johnson, et R. R. Riolo, « Improving rural electricity system planning: An agent-based model for stakeholder engagement and decision making », *Energy Policy*, vol. 101, p. 317-331, févr. 2017, doi: 10.1016/j.enpol.2016.10.020.
[12] E. M. Nfah, J. M. Ngundam, M. Vandenbergh, et J. Schmid, « Simulation of off-grid generation options for remote villages in Cameroon », *Renew. Energy*, vol. 33, n° 5, p. 1064-1072, mai 2008, doi: 10.1016/j.renene.2007.05.045.
[13] S. Szabo, K. Bodis, T. Huld, et M. Moner-Girona, « Energy solutions in rural Africa: mapping electrification costs of distributed solar and diesel generation versus grid extension », *Env. Res Lett*, p. 10, 2011.
[14] M. Moner-Girona *et al.*, « Decentralized rural electrification in Kenya: Speeding up universal energy access », *Energy Sustain. Dev.*, vol. 52, p. 128-146, oct. 2019, doi: 10.1016/j.esd.2019.07.009.
[15] P. K. Ainah et K. A. Folly, « Development of Micro-Grid in Sub-Saharan Africa: an Overview », *Int. Rev. Electr. Eng. IREE*, vol. 10, n° 5, p. 633, oct. 2015, doi: 10.15866/iree.v10i5.5943.

[16] M. E. Khodayar, « Rural electrification and expansion planning of off-grid microgrids », *Electr. J.*, vol. 30, n° 4, p. 68-74, mai 2017, doi: 10.1016/j.tej.2017.04.004.
[17] N. Plain, B. Hingray, et S. Mathy, « Accounting for low solar resource days to size 100% solar microgrids power systems in Africa », *Renew. Energy*, vol. 131, p. 448-458, févr. 2019, doi: 10.1016/j.renene.2018.07.036.
[18] World Bank et ESMAP, « Benchmarking study of solar PV mini grids investment costs », World Bank, déc. 2017. Consulté le: 2 décembre 2021. [En ligne]. Disponible sur: https://documents1.worldbank.org/curated/ru/569621512389752401/pdf/121829-ESM-PVHybridminigridsCostingbenchmarkTTAESMAPConfEdtemplateDecv-PUBLIC.pdf
[19] IRENA, « Solar PV in Africa : costs and markets », IRENA, sept. 2016. Consulté le: 2 décembre 2021. [En ligne]. Disponible sur: https://www.irena.org/-/media/Files/IRENA/Agency/Publication/2016/IRENA_Solar_PV_Costs_Africa_2016.pdf
[20] A. F. Crossland, O. H. Anuta, et N. S. Wade, « A socio-technical approach to increasing the battery lifetime of off-grid photovoltaic systems applied to a case study in Rwanda », *Renew. Energy*, vol. 83, p. 30-40, nov. 2015, doi: 10.1016/j.renene.2015.04.020.
[21] M. Gustavsson et D. Mtonga, « Lead-acid battery capacity in solar home systems—Field tests and experiences in Lundazi, Zambia », *Sol. Energy*, vol. 79, n° 5, p. 551-558, nov. 2005, doi: 10.1016/j.solener.2004.10.010.
[22] I. Nygaard, « Measures for diffusion of solar PV are aligned in technology action plans for 6 countries in the African region », p. 16, 2014.
[23] B. Bollinger et K. Gillingham, « Learning-by-Doing in Solar Photovoltaic Installations », p. 67.
[24] « Predicting the costs of photovoltaic solar modules in 2020 using experience curve models », p. 8, 2013.
[25] IRENA, « The Power to Change: Solar and Wind Cost Reduction Potential to 2025 », 2016.
[26] E. S. Rubin, « A review of learning rates for electricity supply technologies », *Energy Policy*, p. 21, 2015.
[27] B. Nykvist et M. Nilsson, « Rapidly falling costs of battery packs for electric vehicles », *Nat. Clim. CHANGE*, vol. 5, p. 4, 2015.
[28] P. Ciller, F. de Cuadra, et S. Lumbreras, « Optimizing Off-Grid Generation in Large-Scale Electrification-Planning Problems: A Direct-Search Approach », *Energies*, vol. 12, n° 24, p. 4634, déc. 2019, doi: 10.3390/en12244634.
[29] D. Cadilla, « Micro-réseaux photovoltaïques hybrides - Guide de conception et Calcul », Ecowas Center for Renewable Energy and Energy Efficiency (ECREEE), juill. 2017.
[30] G. Léna, « Mini-réseaux hybrides PV-diesel pour l'électrification rurale », International Energy Agency, juill. 2013.
[31] C. Ashton et M. Siira, « IEEE Recommended Practice for Sizing Stand-Alone Photovoltaic (PV) Systems », IEEE. doi: 10.1109/IEEESTD.2021.9528316.
[32] D. O. Akinyele et R. K. Rayudu, « Techno-economic and life cycle environmental performance analyses of a solar photovoltaic microgrid system for developing countries », *Energy*, vol. 109, p. 160-179, août 2016, doi: 10.1016/j.energy.2016.04.061.
[33] C. Smith, « Comparative Life Cycle Assessment of a Thai Island's diesel/PV/wind hybrid microgrid », *Renew. Energy*, p. 16, 2015.
[34] C. Cader, P. Bertheau, P. Blechinger, H. Huyskens, et Ch. Breyer, « Global cost advantages of autonomous solar–battery–diesel systems compared to diesel-only systems », *Energy Sustain. Dev.*, vol. 31, p. 14-23, avr. 2016, doi: 10.1016/j.esd.2015.12.007.
[35] « Nationally Determined Contributions (NDCs) ». https://unfccc.int/process-and-meetings/the-paris-agreement/nationally-determined-contributions-ndcs/nationally-determined-contributions-ndcs (consulté le 21 janvier 2022).
[36] E. Hartvigsson et E. O. Ahlgren, « Comparison of load profiles in a mini-grid: Assessment of performance metrics using measured and interview-based data », *Energy Sustain. Dev.*, vol. 43, p. 186-195, avr. 2018, doi: 10.1016/j.esd.2018.01.009.

[37] N. Plain, « Micro-réseaux d'électricité 100% solaire et isolés en Afrique. Eléments de dimensionnement, coût de l'électricité, dépendance au climat régional et au profil de demande », 2020.
[38] N. J. Williams, P. Jaramillo, B. Cornell, I. Lyons-Galante, et E. Wynn, « Load characteristics of East African microgrids », in *2017 IEEE PES PowerAfrica*, juin 2017, p. 236-241. doi: 10.1109/PowerAfrica.2017.7991230.
[39] U. Pfeifroth *et al.*, « Surface Radiation Data Set - Heliosat (SARAH) - Edition 2 ». Satellite Application Facility on Climate Monitoring (CM SAF), 13 juin 2017. doi: 10.5676/EUM_SAF_CM/SARAH/V002.
[40] H. Hersbach *et al.*, « The ERA5 global reanalysis », p. 51.
[41] E. Lorenz, T. Scheidsteger, J. Hurka, D. Heinemann, et C. Kurz, « Regional PV power prediction for improved grid integration », p. 15, 2010.
[42] E. L. Maxwell, « A Quasi-Physical Model for Converting Hourly Global Horizontal to Direct Normal Insolation », Solar Energy Research Institute, Midwest Research Institute, août 1987.
[43] A. Bahrami, « The effect of latitude on the performance of different solar trackers in Europe and Africa », *Appl. Energy*, p. 11, 2016.
[44] IRENA, « Electricity storage and renewables: Costs and markets to 2030 », 2017.
[45] ESMAP et SE4All, « Beyond Connection - Energy Access Redefined », World Bank, Technical Report, juill. 2015.
[46] U. E. Hansen, M. B. Pedersen, et I. Nygaard, « Review of solar PV policies, interventions and diffusion in East Africa », *Renew. Sustain. Energy Rev.*, vol. 46, p. 236-248, juin 2015, doi: 10.1016/j.rser.2015.02.046.
[47] E. Vartiainen, G. Masson, C. Breyer, D. Moser, et E. Román Medina, « Impact of weighted average cost of capital, capital expenditure, and other parameters on future utility-scale PV levelised cost of electricity », *Prog. Photovolt. Res. Appl.*, vol. 28, n° 6, p. 439-453, juin 2020, doi: 10.1002/pip.3189.
[48] C. Candelise, M. Winskel, et R. J. K. Gross, « The dynamics of solar PV costs and prices as a challenge for technology forecasting », *Renew. Sustain. Energy Rev.*, vol. 26, p. 96-107, oct. 2013, doi: 10.1016/j.rser.2013.05.012.
[49] C. Trimble, M. Kojima, I. P. Arroyo, et F. Mohammadzadeh, « Financial Viability of Electricity Sectors in Sub-Saharan Africa », p. 105.
[50] ESMAP, « Global Solar Atlas ». https://globalsolaratlas.info/map (consulté le 7 mars 2022).
[51] K. Louw, B. Conradie, M. Howells, et M. Dekenah, « Determinants of electricity demand for newly electrified low-income African households », *Energy Policy*, p. 7, 2008.
[52] S. J. Lee, E. Sánchez, A. González-García, P. Ciller, P. Duenas, et J. Taneja, « Investigating the Necessity of Demand Characterization and Stimulation for Geospatial Electrification Planning in Developing Countries », p. 14.
[53] M. Lee, D. Soto, et V. Modi, « Cost versus reliability sizing strategy for isolated photovoltaic micro-grids in the developing world », *Renew. Energy*, vol. 69, p. 16-24, sept. 2014, doi: 10.1016/j.renene.2014.03.019.
[54] M. Lacirignola, P. Blanc, R. Girard, P. Pérez-López, et I. Blanc, « LCA of emerging technologies: addressing high uncertainty on inputs' variability when performing global sensitivity analysis », *Sci. Total Environ.*, vol. 578, p. 268-280, févr. 2017, doi: 10.1016/j.scitotenv.2016.10.066.
[55] A. Goodrich, T. James, et M. Woodhouse, « Residential, Commercial, and Utility-Scale Photovoltaic (PV) System Prices in the United States: Current Drivers and Cost-Reduction Opportunities », NREL/TP-6A20-53347, 1036048, févr. 2012. doi: 10.2172/1036048.
[56] HOMER Energy, « HOMER® Pro Version 3.7 User Manual ». 2016. [En ligne]. Disponible sur: https://www.homerenergy.com/pdf/HOMERHelpManual.pdf
[57] H. Seyedhashemi, B. Hingray, C. Lavaysse, et T. Chamarande, « The Impact of Low-Resource Periods on the Reliability of Wind Power Systems for Rural Electrification in Africa », *Energies*, vol. 14, n° 11, p. 2978, janv. 2021, doi: 10.3390/en14112978.